Dynamics of transient pores in stretched vesicles

Olivier Sandre, Laurent Moreaux, Françoise Brochard-Wyart

Proc. Natl. Acad. Sci. USA
Vol. 96, pp. 10591–10596, September 1999
Physics

Dynamics of transient pores in stretched vesicles

OLIVIER SANDRE*†, LAURENT MOREAUX‡, AND FRANÇOISE BROCHARD-WYART*

*Laboratoire Physico-Chimie Curie–Unité Mixte de Recherche 168 Centre National de la Recherche Scientifique/Institut Curie, 11, rue Pierre et Marie Curie 75248 Paris CEDEX 05, France; ‡Laboratoire de Physiologie–Unité Mixte de Recherche, 7637 Centre National de la Recherche Scientifique/Ecole Supérieure de Physique et de Chimie Industrielles, 10, rue Vauquelin 75231 Paris CEDEX 05, France

Communicated by Pierre-Gilles de Gennes, Ecole Supérieure de Physique et de Chimie Industrielles, Paris, France, July 2, 1999 (received for review June 2, 1999)

ABSTRACT **We image macroscopic transient pores in mechanically stretched giant vesicles. Holes open above a critical radius r_{c1}, grow up to a radius r_{c2}, and close. We interpret the upper limit r_{c2} by a relaxation of the membrane tension as the holes expand. The closing of the holes is caused by a further relaxation of the surface tension when the internal liquid leaks out. A dynamic model fits our data for the growth and closure of pores.**

Opening a hole in a biological membrane has been a challenge for drug delivery and gene therapy. Chemical strategies, based on the addition of a suitable agent (1, 2) [detergent proteins such as talin (3)] and physical means (4) [electroporation (5), osmotic shock (6), temperature jump (4), and adhesion on porous (7) or decorated substrates (8) (A. L. Bernard, M. A. Guedeau-Boudeville, O.S., S. Palacin, J. M. diMiglio, and L. Jullien, unpublished data), have been developed to increase membrane permeability.

Our approach is to stretch the vesicle membrane: even a weak adhesion or an intense light provides a tension σ, which relaxes by the formation of transient macroscopic pores. The standard difficulty of visualizing directly at video rate the fast dynamics of pore openings and closings is overcome here by the use of a viscous solvent. The role of solvent viscosity is surprising: under tension, vesicles start to burst, very much like viscous bubbles (9), and this is controlled by lipid viscosity. However, as we shall see, there is a leak-out of the internal liquid, which relaxes the tension and induces the closure of the pore. In a solution of low viscosity (like water), leak-out is fast: the pores close before reaching a visible size. If we make the solvent more viscous, leak-out is slowed down: the pores reach sizes up to 10 μm. The immersion of vesicles in a viscous environment allows visualization of transient pores in a membrane stretched by either intense illumination or weak adhesion on a solid substrate.

For clarity, we begin by presenting in the next section a simple theoretical picture of the pore's dynamics. After that, we describe the experiments.

Model of the Opening and Closing of Pores. Closed membranes, such as red blood cells or vesicles, are under zero surface tension in their equilibrium unswollen phase (10). They undulate by thermal fluctuations. The resistance to deformations of the membrane is mainly caused by curvature energy. The surface is crumpled, as shown in Fig. 5*a*. An excess area $\Delta A = A - A_p > 0$ (where A is the total area and A_p the projected area) is required to maintain the zero surface-tension state (11–13). When a vesicle adheres to a substrate or is sucked in a glass micropipette, the surface cannot adjust to its optimal value, and a surface tension of σ is created. The fluctuations of the membrane are strongly reduced, and the shape of the vesicle becomes spherical (Fig. 5*b*). The micropipette technique allows one to measure the relation between the tension σ (over four decades, 10^{-3}–10 mN/m) and the increase of the projected area A_p (14). Two regimes appear in the stretching of the crumpled membrane: (*i*) a low-tension regime, where the shape fluctuations are not yet destroyed. The projected area A_p increases logarithmically with σ; (*ii*) a high-tension regime, where A_p increases linearly with tension because of a direct expansion of the area per molecule. The relation between the area strain $\alpha = \Delta A/A]_{\sigma=0} - \Delta A/A]_{\sigma}$, and the tension σ fits the theoretical prediction (15, 16):

$$\alpha \cong \frac{kT}{8\pi\kappa} \ln\left(1 + c\,\frac{\sigma A}{\kappa}\right) + \frac{\sigma}{E}, \qquad [1]$$

where κ and E are the elastic moduli for bending and area expansion, respectively (the coefficient c equals $1/24\pi$ for a spherical closed membrane). The crossover between the two regimes arises at a critical tension $\sigma_c = E\ kT/8\pi\kappa$. Typical estimates for a membrane of thickness d are $E \cong \kappa/d^2$ and $\sigma_c \cong kT/8\pi d^2 \approx 0.1$–1 mN/m.

If a vesicle is in a stretched state, the initial tension σ_0 of the closed membrane is relaxed by the opening of a pore (17). The radius r_c of the hole at which the surface stress is entirely relaxed is derived from Eq. **1**: $\pi r_c^2/A \cong kT/8\pi\kappa \ln(1 + c\ \sigma_0 A/\kappa) + \sigma_0/E$.

We describe the dynamics of pores in a membrane by analogy with the opening of holes in viscous bare films (18, 19). The growth law of the hole is derived from a transfer of surface energy into viscous losses:

$$4\pi\eta d\dot{r} = 2\pi r f, \qquad [2]$$

where ηd is the surface viscosity, and $f = 2\gamma$ is the surface tension acting on the film. From Eq. **2**, one finds that the hole radius increases exponentially $r(t) = r_i e^{t/\tau}$, where $\tau = \eta d/2\gamma$, and r_i is the initial radius after nucleation. The growth of pores in tense vesicles is more complex, because (*i*) the tension of the membrane relaxes to zero as a pore expands (10), and (*ii*) the line tension cannot be neglected. It is the driving force to close the pores. Including these two effects, we write the driving force f per unit length of the hole as

$$f = \sigma_0\left(1 - \frac{r^2}{r_c^2}\right) - \frac{\Im}{r}, \qquad [3]$$

where σ_0 is the membrane tension before the opening of the hole. The first term describes that the surface tension decreases linearly with the area of the pore. This assumption becomes exact in the two limits (*i*) of high tension ($\sigma > \sigma_0$) with $\sigma_0 = \pi r_c^2/A\ E$ and (*ii*) of very low tension ($\sigma \ll \kappa/A$) when the membrane is strongly fluctuating, but now the relation between σ_0 and r_c is $\sigma_0 = 24\pi\kappa\ \pi r_c^2/A^2\ 8\pi\kappa/kT$. The second term in Eq. **3** is the restoring force that tends to close the pore because the line energy $\Im$ per unit length. Because $\Im$ originates from the energetic cost to curve the lipid molecules at the edges of the pore, it is of order of $\kappa/2d$ ($\approx 10^{-11}$ *N*). The plot of the driving force vs. r is shown in Fig. 1: f is positive, i.e. the hole grows, in a range $r_{c1} < r < r_{c2}$. Below r_{c1} ($r_{c1} \cong \Im/\sigma_0$), the line energy overcomes the gain of surface

The publication costs of this article were defrayed in part by page charge payment. This article must therefore be hereby marked "*advertisement*" in accordance with 18 U.S.C. §1734 solely to indicate this fact.

PNAS is available online at www.pnas.org.

A Commentary on this article begins on page 10550.

†To whom reprint requests should be addressed. E-mail: Olivier.Sandre@curie.fr.

energy, and the pore closes. Above r_{c1}, the pore will grow to $r = r_{c2}$ ($r_{c2} \cong r_c - r_{c1} \approx r_c$) and stop. The life of a transient pore presents three steps:

Step 1: Growth. The growth of a hole larger than r_{c1} is ruled by Eq. **2** with $f \cong \sigma(r) = \sigma_0(1 - r^2/r_c^2)$. This leads to:

$$\ln \frac{r}{r_i} - \frac{1}{2} \ln \frac{r_c^2 - r^2}{r_c^2 - r_i^2} = \frac{t}{\tau}, \qquad [4]$$

where $\tau^{-1} = \sigma_0/\eta d$.

Step 2: Leak-out of the internal liquid. The tension of the vesicle $\sigma(r)$ leads to an excess Laplace pressure for the fluid inside the vesicle $\Delta P = 2\sigma(r)/R_v$, where R_v is the vesicle radius ($A_p = 4\pi R_v^2$). If a hole of radius r is open, the inside liquid leaks out and decreases σ_0. The curve $f(r)$ is shifted down (Fig. 1), and the pore will close. So we have to compare the leak-out time τ_L to the growth time τ. For a pore of size r, the velocity V_L of leak-out is given by $\eta_0 V_L/r^2 \cong \Delta P/r$, where η_0 is the viscosity of the liquid bath. The flux $Q \cong V_L r^2$ expelled per unit time is $Q \cong \sigma/\eta_0 r^3/R_v$. This leads to a decrease of the internal volume Ω per unit time $d\Omega/dt = -Q$ and to an increase of the excess area $dA \cong A/\Omega\, Q dt$. The time τ_L to release a surface fraction $\Delta A/A$ is then $\tau_L \cong \eta_0/\sigma_0\, \Delta A/A (R_v/r)^3 R_v$. Assuming that the entire surface of the pore is recovered as excess area available for fluctuations leads to $\Delta A/A \cong r^2/R_v^2$ and hence $\tau/\tau_L \cong \eta d/\eta_0\, r/R_v^2$. If the leak-out time τ_L is larger than the rise time τ, the pore radius expands before all the initial tension of the vesicle is relaxed. The condition $\tau = \tau_L$ defines an upper limit for the radius of the pores $r_L \cong \eta_0/\eta d\, R_v^2$. This explains why we are the first to make pictures of the transient pores, the trick being to use a viscous medium (where the viscosity η_0 is increased by a factor of 30, and the maximum size of the pores varies by more than a decade).

Step 3: Closure of pores. The initial tension σ_0 has relaxed to zero by leak-out of the internal solution. Now the pore closes to reduce its line energy. Taking Eq. **2** with $f = -\Im/r$ leads to a decrease of the pore radius at constant velocity:

$$V = -\dot{r} = \frac{\Im}{2\eta d} \qquad [5]$$

MATERIALS AND METHODS

We study giant unilamellar vesicules, which have a membrane composed of a single phospholipidic bilayer. Several methods of optical microscopy can be used to image the tiny membrane: phase contrast, differential interference contrast, reflection interference contrast microscopy (20, 21), and fluorescence microscopy. We use here a hydrophobic fluorescent labeling of the oily chains providing optimal contrast on the membrane. The vesicles are either freely suspended in the liquid medium or attached to a glass substrate by varying the physicochemical conditions. Finally, we test the membrane permeability by monitoring its electrical conductance with a sharp electrode.

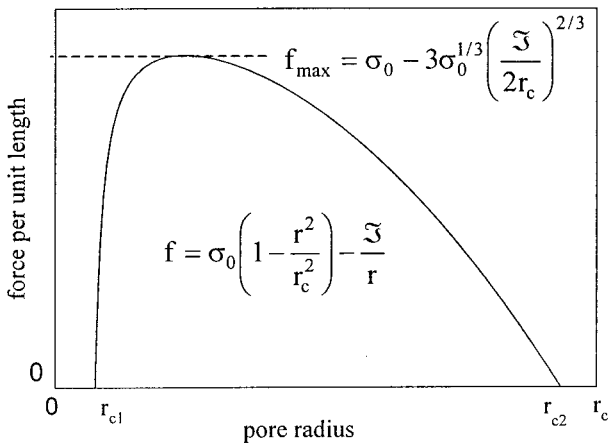

FIG. 1. Force per unit length acting on the pore in a membrane of line energy $\Im$ and initial tension σ_0. The sign is positive, and f tends to expand the pore for radii between r_{c1} and r_{c2}.

Preparation. We use the electroformation method (22), which produces giant unilamellar vesicles with a high efficiency and very few multilamellar aggregates. The bilayer is made of 1,2-dioleoyl-*sn*-glycero-3-phosphocholine (DOPC, Sigma) which is in the fluid phase L_α at room temperature and has been shown to form vesicles in arbitrary mixtures of water and glycerol (23). It is labeled by the lipophilic fluorescent dye N-(3-sulfopropyl)-4-(4-(didecylamino) styryl)pyridinium (Di_{10}ASP-PS), (S-467, Molecular Probes). A solution of pure lipid (1 mg/ml in a chloroform/methanol 2:1 mixture) is spread on both windows of a homemade preparation chamber composed of two transparent electrodes (glass plates coated with indium tin oxide) and a teflon spacer (1-mm thick). After drying (1 h in vacuum), the chamber is filled with 1.5 ml of the aqueous buffer to encapsulate. The ac voltage is set immediately to start the gentle swelling of the lipidic film and avoid spontaneous vesiculation. The conditions of tension and duration are adapted to the osmolarity, conductivity, and viscosity of the solution to encapsulate: 1.1 V at 10 Hz for 2 h with a solution 0.1 M in pure water, 1.5 V at 6 Hz overnight for the same concentration in a water/glycerol mixture. The osmotic pressure is controlled by a concentration of sugar ranging from 0.05 M to 0.3 M, which is either glucose or sucrose, to make a gradient of mass densities between the inner and outer compartments of the vesicles ($\Delta\rho = 0.0162$ g/cm^3 for 0.1 M osmolarity). The maximum electric conductivity is $1.2 \times 10^{-4}\ \Omega^{-1}\ \text{cm}^{-1}$ when the buffer contains 1 mM NaCl, but usually the only electrolyte is 10 mg/l, NaN_3, which is a bactericide. The viscosity of the medium is enhanced by using a mixture of water and glycerol as solvent. The viscosity $\eta_0 = 32.1 \pm 0.4$ centipoise (1 poise = 10^1 Pa·s) is measured with a capillary viscosimeter (Ubbelohde method) for a volume ratio 2:1 glycerol/water and 0.1 M sucrose. A delay of a few hours after switching off the electric field is necessary for the vesicles to exhibit large thermal undulations. The stock suspension of giant unilamellar vesicles is about 0.1 mg/ml lipid ($\approx$130 μM).

Observation. Aliquots of the giant unilamellar vesicles suspension are incubated with 1% v/v of 560 μM Di_{10} ASP-PS in ethanol for half an hour in order to insert the dye at 4 mol% into the DOPC bilayers. Then they are diluted and in some cases settled in two volumes of equiosmolar solution. The samples are observed in a closed chamber (two glass slides spaced by 200 μm and sealed with hot paraffin) to avoid streams caused by evaporation. A conventional upright fluorescence microscope with an immersion objective [×100/1.25 oil Zeiss Achroplan or ×63/0.90 water Olympus (New Hyde Park, NY) LUMPlanF1] and a motorized focus is used. Excitation in epiillumination is provided by a 200-W mercury lamp through a 455-490-nm band pass filter, and the fluorescence (peak at 580 nm) is detected with a standard

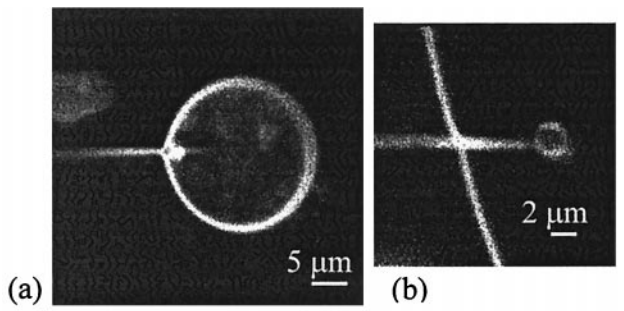

FIG. 2. (*a*) Sharp electrode introduced inside an adhering vesicle that contains sucrose and 1 mM NaCl for electrical conductivity. The membrane reseals tightly around the glass pipette, so that the current lines (10 pA) are confined though the lipidic bilayer. (*b*) enlargement for another vesicle showing the tip end plugged by a small vesicle.

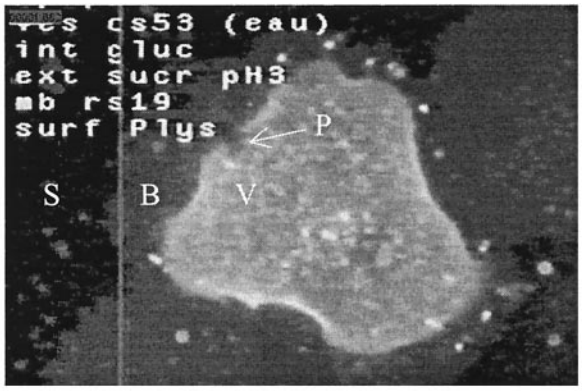

(a)

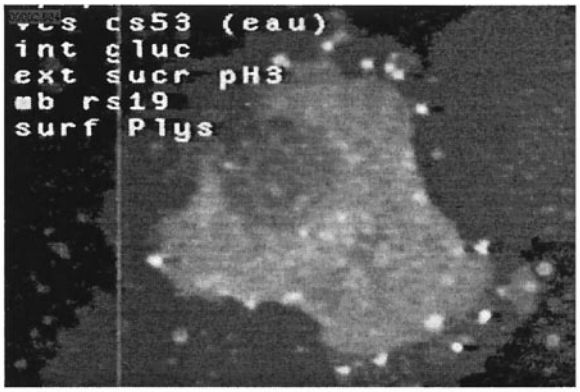

(b)

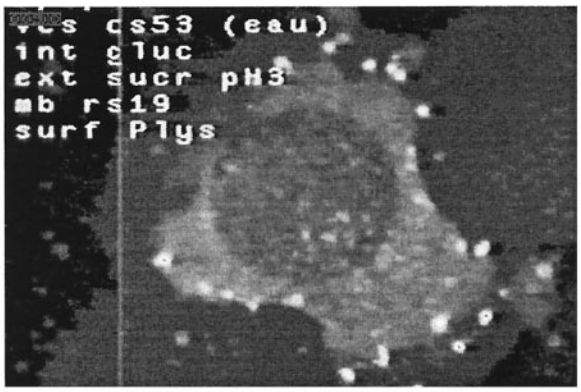

(c)

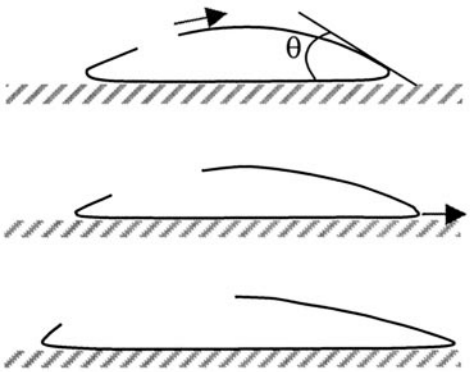

(d)

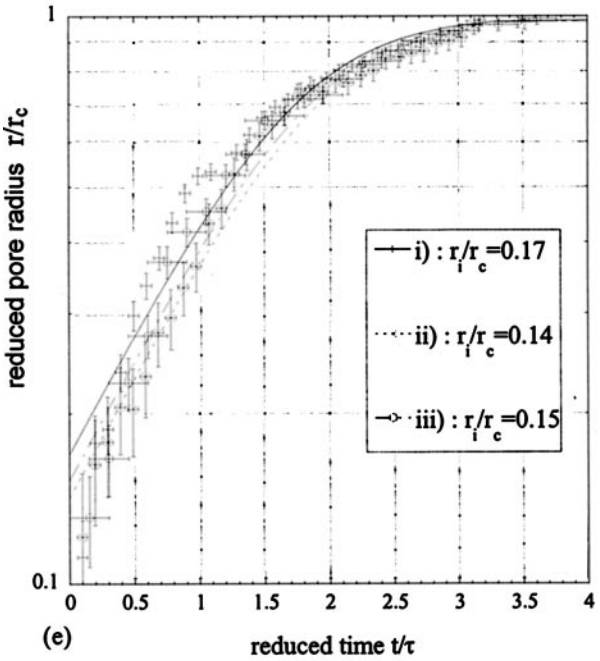

(e)

FIG. 3. Bursting pores in strongly adhering vesicles; the substrate is treated with poly(L-lysine) the solution is acidic (pH 3) and has a low viscosity $\eta_0 \approx 1$ cpoise; (*a–c*) time sequences; (*d*) sketch of bursting and spreading; (*e*) growth of pores and fits in reduced units (t/τ vs. r/r_c) using Eq. **4** for three different vesicles leading to: (*i*) $\tau = 1.01 \pm 0.05$ s, $r_i = 1.9 \pm 0.1$ μm, $r_c = 11.3 \pm 0.1$ μm; (*ii*) $\tau = 1.02 \pm 0.04$ s, $r_i = 0.80 \pm 0.05$ μm, $r_c = 5.6 \pm 0.05$ μm; (*iii*) $\tau = 0.27 \pm 0.01$ s, $r_i = 1.3 \pm 0.1$ μm, $r_c = 8.4 \pm 0.05$ μm. Curve *i* corresponds to the pore shown in *a–c*.

charge-coupled device camera. The pictures are digitized on an 8-bit frame grabber (LG-3, Scion, Frederick, MD) and analyzed with IMAGE software (National Institutes of Health). The figures are provided on the PNAS web site as supplemental material with a color look-up table (see www.pnas.org). Photobleaching is very slow, especially in the mixed glycerol/water solutions, where the fluorescence intensity stays constant under continuous illumination of the sample for up to 1 h.

Adhesion. Depending on the experiment, the glass slides of the observation chamber are either bare or are treated with an

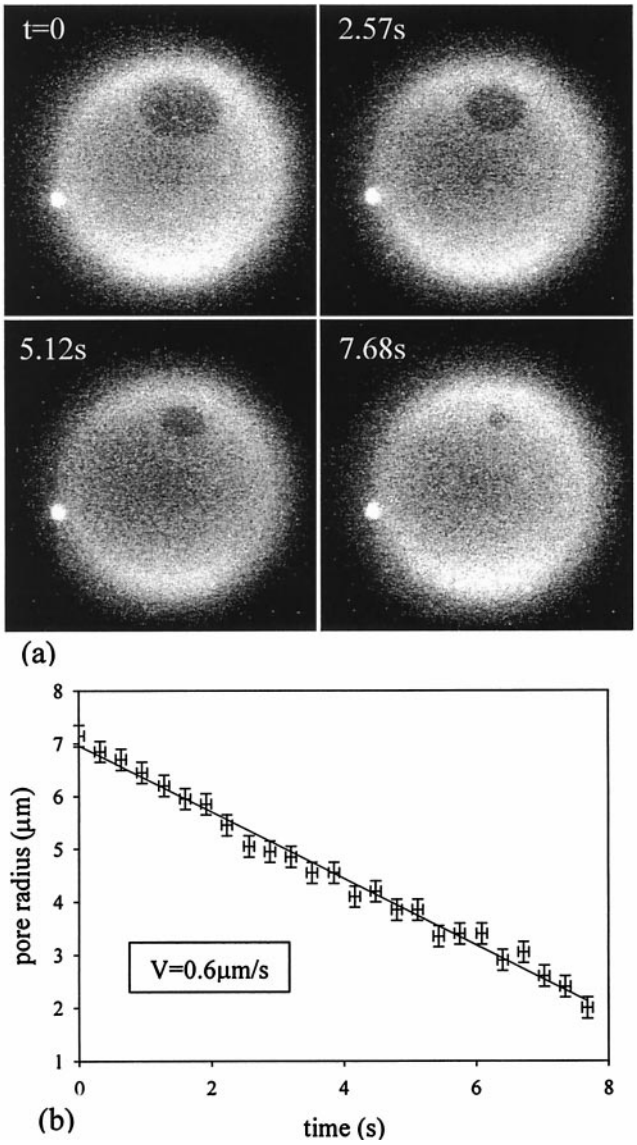

FIG. 4. (*a*) Time sequences of a pore closure in a vesicle tensed by intense illumination. Addition of glycerol raises the viscosity up to $\eta_0 \approx 32$ cpoise and slows down the leaking of the inner liquid, which enables to observe macroscopic transient pores; (*b*) the radius decreases at constant velocity V.

adhesive coating for the vesicles. In all cases, they have been cleaned with an alkaline detergent (Decon 90, Prolabo, Fontenay-sous-bois, France) followed by abundant rinsing with ultrapure water and drying under nitrogen. Gravity is used to favor the contact between the vesicles and one slide (either bottom or top, depending on the sign of the sugar gradient). In addition, an electrostatic attraction promotes the adhesion of the bilayer to the glass. Two methods have been investigated. The first consists of incubating the aliquots of vesicles with a glucose solution containing 1 mM $CaCl_2$. As a divalent cation, calcium adsorbs strongly to the phosphatidylcholine headgroups of the bilayers, thus conferring to the vesicles a net positive charge. Therefore they are attracted by the weakly negative surface of bare glass at neutral pH. The second method is to adsorb polycationic chains onto the glass substrates. We use for that purpose a solution of 0.01% w/v poly(L-lysine) ($M_w \approx 150{,}000$, P8920, Sigma) intended for adhering tissue sections to glass slides. The intensity of the electrostatic interaction can be modulated by the calcium concentration in the former case and by the pH-dependent charging of the ammonium residues in the latter. An effective contact angle θ can be defined by analogy with wetting (Fig. 3*d*) and is measured experimentally. Weak adhesion is associated arbitrarily to $\theta > 90°$ and strong adhesion to $\theta < 90°$.

Electrical Measurements. In order to characterize the permeability of the vesicles, we introduce a sharp electrode into the inner compartment and apply a pulse of current (10–100 pA) to follow the charge and discharge of the membrane. This requires an open cell, with the vesicles adhering at the bottom. Glass capillaries (Glark Electromedical Instruments, Pangbourne, UK) are pulled with a microforge to make tips having an outer radius of less than 1 μm at their end. They are filled with a water-soluble fluorescent dye (1 mM calcein, pH 7.4) for convenient observation and with 1 M KCl for electrical conductivity. The pipette is held by a micromanipulator. The counterelectrode is a silver wire, and the circuit is closed by an intracellular recording amplifier (model IR-283, Neurodata Instruments, Delaware Water Gap, PA). The resistance of a pipette has a typical value of 100 MΩ. A simple calculation gives $R_{\text{tip}} = (\gamma_{\text{KCl}} \pi \alpha r_{in})^{-1}$, where $\gamma_{\text{KCl}} \approx 10^{-2}\ \Omega^{-1}\ \text{cm}^{-1}$, and the angle of the tip $\alpha \approx 1°$ is measured. This leads to an inner radius at the end of the tip $r_{\text{in}} \approx 200$ nm.

RESULTS

Electrical Measurements. In of Fig. 2 *a* and *b*, it appears that the bilayer reseals after being pierced by the sharp electrode. A negative current (10 pA) must be applied continuously to repel the lipid membranes and impede the plugging of the tip. Therefore, the fixation of the vesicle on the substrate makes the experiments easier because it spares a second holding pipette. A pulse of 200 ms duration and 10 pA amplitude is superimposed on the dc current. The voltage measured between the two aqueous compartments of the vesicle is the classical response of charge and discharge of a capacitor. In particular, the relaxation time τ_e is in the range 10–30 ms and is proportional to the vesicle surface area. The voltage that can be maintained across the bilayer gives the leaking conductance G of the membrane. We focus our attention here on the variation of G with the strength of adhesion. A freely suspended vesicle has a low conductance $G = G_{in} \approx 10^{-10}\ \Omega^{-1}$ attributed to the nonzero permeability of the bilayer to the electrolyte (NaCl). When stuck to the substrate, a vesicle has an increased conductance written as $G = G_m + G_{\text{p}}$, where G_{p} is the conductance through one or more pores. This contribution is $G_{\text{p}} = 1 - 1.5 \times 10^{-10}\ \Omega^{-1}$ for vesicles adhering on glass by adsorption of divalent cations in 0.5 mM $CaCl_2$. It increases up to $G_{\text{p}} = 2 - 4 \times 10^{-10}\ \Omega^{-1}$ in 1 mM $CaCl_2$. The adhesion on glass covered with poly(L-lysine) leads to $G_{\text{p}} = 9 \times 10^{-10}\ \Omega^{-1}$ at pH 6.6 and $G_{\text{p}} = 24 \times 10^{-10}\ \Omega^{-1}$ at pH 4.3. The adhesion strength (evaluated from the effective contact angle of the vesicle on the substrate) is indeed larger with poly(L-lysine) than with calcium, and increased respectively at lower pH and larger $CaCl_2$ concentration. Thus it is clear that G_{p} increases when the vesicle adheres more strongly to the substrate. This increased permeability is a first evidence for the presence of transient pores in the membrane, with a size or a number that increases when the vesicle is under more mechanical tension. These pores have a size below optical resolution.

Bursting of a Pore in Vesicles Adhering Strongly to the Substrate. The vesicles have been prepared in an aqueous solution of 0.05 M glucose and diluted in 0.05 M sucrose. The suspension is acidified with hydrochloric acid down to pH 3, and the vesicles are allowed to settle on a glass slide covered by poly(L-lysine). Once adhering on the surface, they appear as flat spherical caps or sometimes more distorted shapes reflecting the chemical heterogeneity of the surface. A few minutes after contact, a macroscopic pore P (radius about 1 μm) nucleates in the vicinity of the wedge (Fig. 3*a*). After a short delay (always less than 1 s), the pore suddenly grows. It appears in the fluorescent membrane as a dark circular hole of increasing radius. Simultaneously, a fluorescent patch of uniform intensity grows around the vesicle V. This lipidic material is a single bilayer B spreading on the substrate S (see the sketch in Fig. 3*d*). From the video-rate recording of the hole expansion, we extract the radius $r(t)$ of the

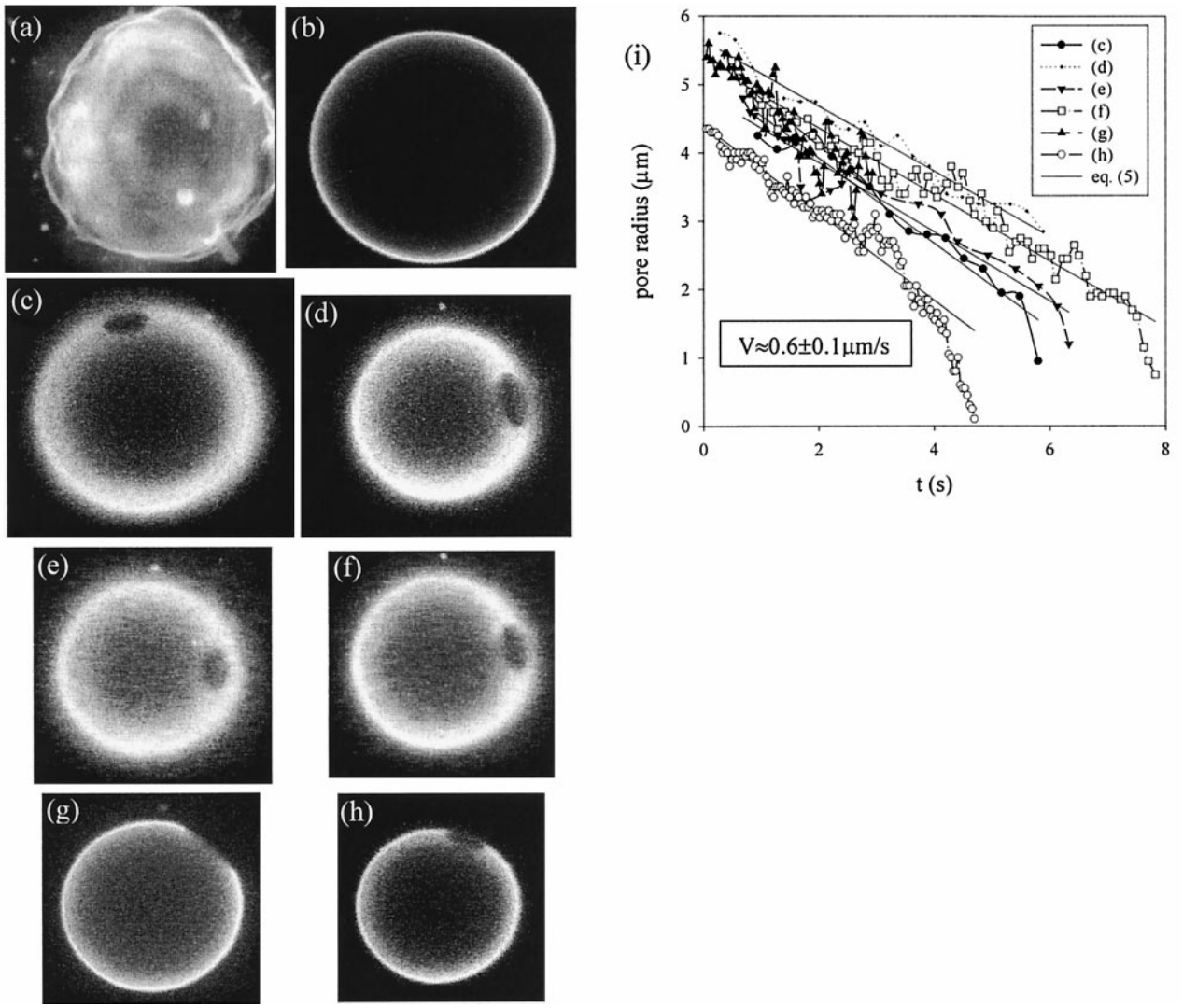

FIG. 5. Vesicle freely suspended in a viscous medium, at first fluctuating (*a*), tense after a while (*b*), then showing a series of transient pores at different locations (*c–h*); pore radii decreasing at constant velocity $V(i)$.

hole vs. time. We fit the plot $r(t)$ using Eq. **4** with three parameters: a characteristic raise time τ, an initial pore radius r_i, and a critical pore size r_c. The growth of pores in three different vesicles is plotted in reduced units of time t/τ and radius r/r_c. All curves are well superimposed (the third parameter r_i/r_c is almost identical for the three vesicles and equals about 0.155). The data are thus in good agreement with Eq. **4**.

Closure of Transient Pores in a Vesicle Tensed by Intense Illumination. The vesicle of Fig. 4 encapsulates a 0.1 M sucrose solution in a viscous mixture of water and glycerol (1:2 v/v). It is suspended in an equimolar solution of glucose. The surface is adhesive (poly(L-lysine adsorbed on glass), but when this pore is present, the vesicle has not yet settled to the bottom slide of the observation chamber. Indeed, the tension originates from the illumination of the fluorescent probe. The pore radius is defined as the long semiaxis of the elliptical projection of the pore in the plane of focusing. Its linear decrease as a function of time is followed by videomicroscopy: the closure velocity is $V = 0.63$ μm/s. In such experiments, up to several tens of transient pores can be observed successively before the vesicle is completely deflated. The typical scenario that leads to a series of transient pores occurring in the same vesicle is depicted on Fig. 5. The vesicle is freely suspended in a viscous medium identical to the encapsulated solution: 0.1 M sucrose in water-glycerol 1:2 (v/v). At first, the membrane exhibits large thermal undulations as observed on view *a*, which is the projection of 100 fluorescence cross sections. Notice the very detailed floppy shape of the vesicle, which had not been detected up to now: our use of a viscous solvent slows down the fluctuations. Thus we obtain an excellent snapshot of the vesicle. After about 10 min of constant illumination, the tension increases and the vesicle becomes perfectly spherical (*b*). Then a series of transient pores produces the slow and discontinuous leaking of the inner solution. The radius R_v of the vesicle decreases progressively after the successive pore events: 22.8 μm (*c*), 18.6 μm (*d*), 18.2 μm (*e*), 17.6 μm (*f*), 17.1 μm (*g*), and 15.9 μm (*h*). Each pore opens in less than 0.1 s and closes in a few seconds. The pore radius is measured as a function of time. The dynamics fits with a constant velocity V: 0.62 μm/s (*c*), 0.48 μm/s (*d*), 0.51 μm/s (*e*), 0.49 μm/s (*f*), 0.69 μm/s (*g*), and 0.64 μm/s (*h*). However, one notes that there is almost always an acceleration in the final stage near zero radius. In the limit of the experimental uncertainty, the value of the closure velocity is reproducible on several pores and equals $V \approx 0.6 \pm 0.1$ μm/s for this given vesicle.

Closure of Transient Pores in a Vesicle Stretched by Weak Adhesion. In Fig. 6, the same 0.1 M glucose solution in water-glycerol (1:2) is encapsulated and is used as the suspending medium outside. The glass surface is treated with poly(L-lysine). Initially a radius $R_v = 19.4$ μm is measured at the equator of the vesicle. At that time, the radius of the contact area measured in the plane of the solid surface is $R_c = 13.9$ μm, corresponding to an effective contact angle $\theta \approx 135°$ (in the convention of wetting).

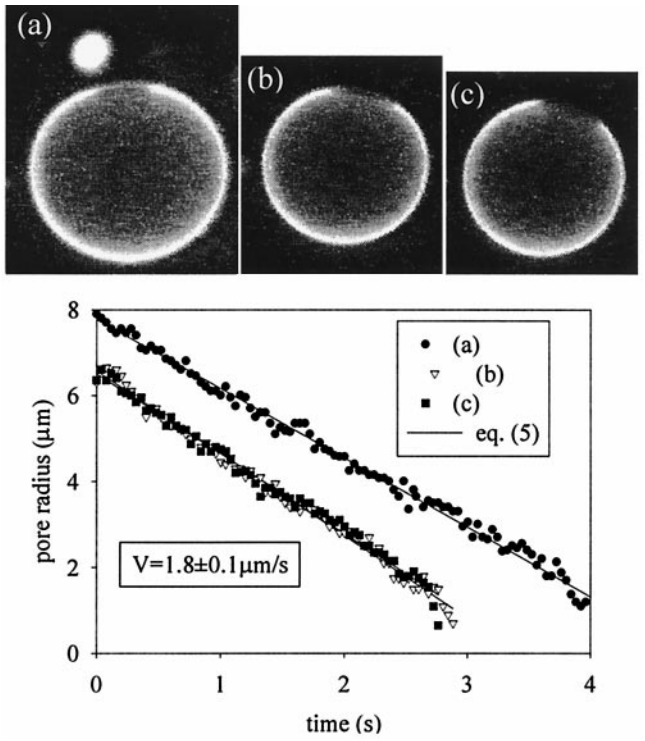

FIG. 6. Series of three transient pores (*a*–*c*) in a vesicle adhering weakly on the substrate poly(L-lysine) on glass, viscous solution without acid).

This value is compatible with the regime of weak adhesion (24). Because of leaking through the pores, R_v decreases with time: 19 μm (*a*), 17.4 μm (*b*), and 15.9 μm (*c*). Unlike in experiments with strong adhesion, the pores do not cause the spreading of the vesicle onto the surface. The hot spot near the vesicle on view *a* is a lipid aggregate that is expelled by the leak-out though the pore. It gives a value for the outflow $Q = 420\ \mu m^3/s$ (initial values of the drift velocity and pore radius are, respectively, $V_L = 2.5\ \mu m/s$ and $r = 7.3\ \mu m$) and a crude estimation of the surface tension of the adhering vesicle $\sigma \approx 10^{-3}$ mN/m ($Q \cong \sigma/\eta_0 r^3/R_v$).

DISCUSSION

Our model fits both the opening and closure of pores. We have assumed that friction in the membrane is dominant over viscous dissipation in the surrounding liquid. This implies $\eta d > \eta_0 r$, where η_0 is the viscosity of the ambient medium. In the opposite limit, the force balance will be written as $\eta_0 \dot{r} \cong \sigma_0(1 - r^2/r_c^2) - \Im/r$. It would lead to the growth of holes at a constant velocity σ_0/η_0 (25) and to the closure linear in square root of time. Both of these laws clearly disagree with the experimental data. The surface viscosity estimated from the closure velocity of the pores $\eta d = \Im/2V \approx 5 \times 10^{-6}$ Pa·s·m is indeed larger than $\eta_0 r \approx 3 \times 10^{-7}$ Pa·s·m. From our model and experiments, we deduce the bulk viscosity of the 1,2-dioleoyl-*sn*-glycero-3-phosphocholine bilayer $\eta \approx 5 \times 10^{-6}/4 \times 10^{-9} \approx 10^3$ Pa·s (10^4 poise). It is two orders of magnitude higher than the shear viscosity $\eta_s \approx 10$ Pa·s (10^2 poise) obtained from the diffusion constant of molecular probes in lipidic bilayers $D \approx 10^{-13} - 10^{-12}\ m^2/s$ (23). For comparison, the viscosity of phospholipidic monolayers at the water/air interface ranges from 5×10^2 to 5×10^4 poise (26). The exponential growth of pores at short times gives both the raising time τ and the initial radius r_i. If we identify $r \approx 1\ \mu m$ to $r_{c1} \cong \Im/\sigma_0$, we obtain an estimate $\sigma_0 \approx 10^{-2}$ mN/m. This value of σ_0 for strong adhesion agrees with similar measurements (27) and is one order of magnitude larger than the tension estimated previously for weakly adhering vesicles. The bursting is irreversible: the lipid spreads on the substrate and maintains the membrane under tension. However, the growth law of the pore is not affected, because bursting is faster than spreading.

The stretching of a vesicle by continuous illumination has led to a series of transient pores successively opening and closing. Once the tension has relaxed after the closure of a pore, it must increase again so that another pore nucleates. A tentative explanation is that a fraction of the membrane has been extracted in the form of lipid-dye complexes by the illumination.

CONCLUSION

We have seen transient pores in tense vesicles immersed in a viscous ambient liquid. The pores relax the membrane tension. If the leak-out of the internal liquid (induced by the excess Laplace pressure) could be entirely suppressed, the pore would reach a certain equilibrium size r_c (17). In our case of very viscous liquid, the leak-out is not suppressed but considerably slowed down: the pore opens up to a large radius ($\approx$5–10 μm) and ultimately closes when leak-out has suppressed the surface tension.

For a liquid of low viscosity like water, leak-out becomes fast and limits the size of the transient pores. Our estimates of the two characteristic times (growth and leak-out) show that the maximal pore size is proportional to the viscosity of the ambient liquid. Thus, in water, the transient pores should be small ($\approx$0.5 μm) and short lived. Although they cannot be seen by fluorescence microscopy, their presence is revealed by the increased electrical conductance of the membrane. They may also play a role in the penetration of active molecules through lipid bilayers. Indeed, the permeability of water through a lipidic bilayer—deduced from the deflating of tense-shaped vesicles stuck on a plate—has been found to be larger than expected by a factor 10^8 (28). The authors conclude that some invisible pores must be present when the vesicle is stretched by adhesion.

Our technique of preparing vesicles in an ultraviscous solution may open a new field. Short-time membrane rearrangements (involved in vesicle fusion, endocytosis, exocytosis, and shape changes of the endoplasmic reticulum in cells, etc.) might be examined by fluorescence microscopy in the near future.

We thank M. A. Guedeau-Boudeville and J. Mertz for their advice and encouragement.

1. Remy, J. S., Kichler, A., Mordvinov, V., Schuber, F. & Behr, J. P. (1995) *Proc. Natl. Acad. Sci. USA* **92,** 1744–1748.
2. Ledley, F. D. (1995) *Hum. Gene Ther.* **6,** 1129–1144.
3. Saitoh, A., Takiguchi, K., Tanaka, Y. & Hotani, H. (1998) *Proc. Natl. Acad. Sci. USA* **95,** 1026–1031.
4. Lasic, D. D. (1993) in *Liposomes: From Physics to Applications* (Elsevier, Amsterdam), pp. 318–321.
5. Moroz, J. & Nelson, P. (1997) *Biophys. J.* **72,** 2211–2216.
6. de Gennes, P. G. & Taupin, C. (1982) *J. Phys. Chem.* **86,** 2294–2304.
7. Guedeau-Boudeville, M. A., Jullien, L. & di Miglio, J. M. (1995) *Proc. Natl. Acad. Sci. USA* **92,** 9590–9592.
8. Rahul Singhvi, G. P., Amit Kumar, G. P., Lopez, G. P., Stephanopoulos, G. N., Wang, D. I. C., Whitesides, G. M. & Ingber, D. E. (1994) *Science* **264,** 696–698.
9. Debrégeas, G., de Gennes, P.-G. & Brochard-Wyart, F. (1998) *Science* **279,** 1704–1707.
10. Brochard, F. & Lennon, J.-F. (1975) *J. Phys. I* **36,** 1036–1047.
11. Brochard, F., de Gennes, P. G. & Pfeuty, P. (1976) *J. Phys. I* **37,** 1099–1104.
12. David, F. & Leibler, S. (1991) *J. Phys. II* **1,** 959–976.
13. Seifert, U. (1995) *Z. Phys. B* **97,** 299–309.
14. Evans, E. & Rawicz, W. (1990) *Phys. Rev. Lett.* **64,** 2094–2097.
15. Helfrich, W. & Servuss, R.-M. (1984) *Nuovo Cimento* **3D,** 137–151.
16. Milner, S. & Safran, S. A. (1987) *Phys. Rev. A At. Mol. Opt. Phys.* **36,** 4371–4379.
17. Sens, P. & Safran, S. A. (1998) *Europhys. Lett.* **43,** 95–100.
18. Debrégeas, G., Martin, P. & Brochard-Wyart, F. (1995) *Phys. Rev. Lett.* **75,** 3886–3889.
19. Diederich, A., Bähr, G. & Winterhalter, M. (1998) *Langmuir* **14,** 4597–4605.
20. Rädler, J. & Sackmann, E. (1993) *J. Phys. II* **3,** 727–747.
21. Wiegand, G., Neumaier, K. R. & Sackmann, E. (1998) *Appl. Opt.* **37,** 6982–6905.
22. Angelova, M. I., Soléau, S., Méléard, P., Faucon, J. F. & Bothorel, P. (1992) *Prog. Colloid Polym. Sci.* **89,** 127–131.
23. Orädd, G., Wikander, G., Lindblom, G. & Johansson, L. B.-Å. (1994) *J. Chem. Soc. Faraday Trans.* **90,** 305–309.
24. Albersdörfer, A., Bruinsma, R. & Sackmann, E. (1998) *Europhys. Lett.* **42,** 227–231.
25. Joanny, J. F. & de Gennes, P. G. (1987) *Physica A* **147,** 238–255.
26. Gaines, G. L. (1966) in *Insoluble Monolayers at Liquid-Gas Interfaces*, ed. Prigogine, I. (Wiley, New York), p. 200.
27. Nardi, J., Bruinsma, R. & Sackmann, E. (1998) *Phys. Rev. E Stat. Phys. Plasmas Fluids Relat. Interdisp. Top.* **58,** 6340–6354.
28. Bernard, A.-L. (1999) Ph.D. thesis (University of Paris VI, Paris, France).